THE AMERICAN MINERALOGIST, VOL. 52, NOVEMBER-DECEMBER, 1967

THE MINERALOGY OF THINGMULI, A TERTIARY VOLCANO IN EASTERN ICELAND

IAN S. E. CARMICHAEL, *Department of Geology and Geophysics, University of California, Berkeley.*

ABSTRACT

A series of olivine-tholeiite, basaltic-andesite, icelandite and pitchstone lavas and dykes which make up a Tertiary central volcano in eastern Iceland have been examined mineralogically with the electron-probe. The composition of the coexisting one-phase magnetites and ilmenites has been used to determine the temperatures and oxygen fugacities of their equilibration. These data, for the rocks which contain oxide microphenocrysts, indicate that the tholeiites have liquidus temperatures near 1080°C, falling to 925°C for a porphyritic pitchstone; the oxygen fugacities of the series approximate to those defined by the synthetic fayalite-magnetite-quartz buffer. The groundmass pyroxenes in the basalts and basaltic-andesites are augites and pigeonites which vary in composition in a similar way to those of the Skaergaard intrusion; olivine apparently shows an analogous recurrence of crystallization to the Skaergaard, reappearing in the icelandites as an iron-rich phenocrystic phase and being absent in the tholeiites and basaltic-andesites. The groundmass plagioclase becomes progressively more sodic in the basalts and basaltic-andesites, and its range of zoning becomes increasingly restricted with increase in the amount of the glassy residuum. Of the secondary minerals, only chlorophaeite is sufficiently abundant for analysis and its analyses show some response to the composition of the rocks in which it is found.

INTRODUCTION

The Tertiary flood basalt sequence of eastern Iceland has been interrupted throughout its development by centralized volcanic activity, one aspect of which is the irruption of acid magma as lavas, cone-sheets and small intrusions. The main lava types forming part of one of these volcanoes, Thingmuli, are olivine-tholeiite, olivine-free tholeiite, basaltic-andesite and icelandite together with pitchstones and finely crystalline rhyolites. The petrology of this series has already been described (Carmichael 1964), but at the time of that account very little was known of the chemistry of the constituent minerals of the rocks; this paper seeks to remedy this lack of information.

The lavas are characteristically fine-grained and contain only sporadic phenocrysts of which plagioclase is predominant. Their mineralogy is simple, as pyroxene, plagioclase, occasional olivine and notable amounts of the iron-titanium oxides are the essential constituents of all but the acid rocks. An iron-rich glassy residuum or its alteration product is common and becomes progressively more conspicuous as the silica contents of the rocks increase; it is invariably interstitial to the groundmass feldspar and pyroxene to which, in all but the most acid rocks, it is very subordinate.

Lavas and dykes believed to be accumulative in olivine and plagioclase

TABLE 1. ANALYSES OF TITANIFEROUS MAGNETITES AND CHROMITE

	1 (H.128)	2 (H.6)	3 (G.101)	4 (G.200)	5 (G.146)	6 (G.99)	7 (G.244)	9 (G.84)
	unmixed	unmixed	unmixed	1-phase	1-phase	1-phase	1-phase	1-phase
SiO_2	0.12	0.10	0.09	0.11	0.15	0.25	0.21	0.23
TiO_2	10.2	8.1	28.8	26.7	26.4	27.2	26.7	27.1
Al_2O_3	1.38	2.34	1.18	1.12	1.61	1.29	1.06	1.22
Cr_2O_3	0.05	0.04	0.02	0.02	0.02	*	*	0.03
V_2O_3	1.95	2.00	0.97	0.89	1.01	1.04	0.90	0.71
FeO	80.2	80.3	65.7	66.5	66.7	66.3	66.2	67.0
MnO	0.34	0.19	0.82	1.03	0.68	0.96	1.03	0.83
MgO	1.22	1.13	0.50	0.72	0.13	0.03	0.22	0.19
CaO	0.14	0.13	0.14	0.18	0.18	0.04	0.36	0.19
ZnO	0.06	0.11	0.12	0.07	0.12	0.06	0.08	0.12
Sum	95.7	94.4	98.3	97.3	97.0	97.2	96.8	97.6
				Recalculated analyses				
Ilmenite basis								
Fe_2O_3	53.1	53.9	29.9	32.4	31.4	30.6	31.6	31.6
FeO	32.4	31.8	38.7	37.3	38.4	38.8	37.7	38.5
Total	101.0	99.8	101.2	100.5	100.1	100.8	99.9	100.7
Ulvospinel basis								
Fe_2O_3	46.2	48.4	10.7	14.5	13.7	12.2	13.7	13.4
FeO	38.6	36.7	56.1	53.4	54.4	55.3	53.9	55.0
Total	100.3	99.2	99.4	98.7	98.4	98.4	98.2	99.0
Molecular percent ulvospinel	29.7	23.3	80.9	75.7	75.4	78.2	76.8	77.3

* Below limit of sensitivity, 0.02%.

are infrequently found at Thingmuli, but only one of these rocks, a picrite-basalt (No. 25) has been examined in detail.

The lavas and intrusions which form this volcano grade progressively in composition from olivine-tholeiite to acid rocks of which the pitchstones are one representative; this fractionated series, rich in iron and titanium, is considered to have its liquid line of descent controlled in part by iron-titanium oxides which play a varied role in the order of crystallisation. That the rhyolites and pitchstones are derivatives of a basaltic parent, hitherto considered to be necessary solely on the evidence of the feldspar relationships (Carmichael 1963a), has received welcome support from the strontium isotopic results of Moorbath and Walker (1965) who have shown that the basalts and acid rocks of Iceland have similar values of the ratio Sr^{87}/Sr^{86}.

No details of the petrography or chemistry of the Thingmuli series are given here, the reader being referred to the original paper (Carmichael 1964); the numbering of the specimens has not been changed for this paper.

TABLE 1—(*Continued*)

10 (G.163)	11 (G.194)	12 (G.247)	13 (H.20)	14 (H.107)	16 (G.230)	17 (H.96A)	18 (G.151)	25 (G.94)	25 (G.94)
unmixed	unmixed	unmixed	unmixed	unmixed	1-phase	unmixed	1-phase	core	margin
0.12	0.22	0.25	0.18	0.12	0.13	0.21	0.13	0.05	0.22
23.0	14.9	21.6	13.9	18.1	22.8	19.4	21.5	0.71	23.3
0.99	0.81	0.62	0.78	1.15	1.20	0.67	1.15	24.3	1.78
0.03	0.04	*	*	0.02	*	*	*	37.0	0.70
0.44	0.74	0.22	0.45	0.13	*	0.04	*	0.18	1.70
70.1	78.2	71.4	78.6	74.3	71.8	74.2	73.6	23.7	69.2
0.58	0.51	1.29	0.44	0.58	0.94	0.81	0.88	0.20	0.46
0.47	0.33	0.04	0.46	0.86	0.20	0.17	0.32	13.5	1.24
0.14	0.24	0.11	0.27	0.10	0.09	0.13	0.03	*	0.12
0.07	0.11	0.15	0.13	0.09	0.20	0.21	0.23	*	0.07
95.9	96.1	95.7	95.2	95.4	97.4	95.8	97.8	99.6	98.8
				Recalculated Analyses—(*Continued*)					
37.1	48.2	39.1	49.5	44.0	38.5	42.6	40.8	9.7	33.8
36.7	34.8	36.2	34.0	34.7	37.2	35.9	36.9	15.3	38.8
99.6	100.9	99.6	100.1	99.8	101.3	100.1	101.1	100.9	102.2
21.6	38.1	24.5	40.1	31.8	23.2	29.5	26.3	8.8	20.2
50.6	43.9	49.3	42.5	45.7	50.9	47.6	49.9	15.8	51.0
98.0	99.9	98.1	99.2	96.6	99.7	98.7	100.4	100.5	100.8
66.2	43.0	63.0	40.3	52.0	64.7	56.2	60.6	—	64.9

ANALYTICAL TECHNIQUES

The electron-probe analytical techniques for the Fe-Ti oxides have already been described together with the methods used for the recalculation of their analyses to assess their quality (Carmichael 1967). The techniques and the standards used for the analysis of pyroxenes have also been described (*op. cit.*); however, as the pyroxenes of these basaltic rocks may show extensive zoning, a discrimination test of its limit had to be used. The problem was to decide whether the outer zone of pigeonite mantling augite has a sharp junction between two discrete pyroxene compositions or whether there is a continuous gradation between the two varieties. In order to discriminate between these two possibilities, the following technique was used: with the ARL spectrometers tuned to receive Ca, Mg, and Fe radiation, and with a small diameter electron beam (ca. 1 micron), the pyroxene grain was analyzed. If the calcium counts indicated a composition somewhere between the common values of augite and pigeonite in the rock (an uncommon event), then the pyroxene sample was moved 1 diameter of the electron beam and then reanalyzed for Ca, Mg, and Fe. Invariably, the counts indicated either a normal augite or pigeonite, so that it is considered that within the resolution of the electron beam (1 micron) the augite is mantled by pigeonite (which is also found as independent grains) with a compositional break between them. It is possible that there is a gradational relationship, but if so, it is not detectable within the resolution of the technique. Hereafter it is assumed that two distinct pyroxene phases are present in all those rocks which contain a calcium-rich and a calcium-poor pyroxene, with a miscibility gap between them. For each point of analysis of an unknown pyroxene, the com-

TABLE 2. ANALYSES OF ILMENITES

	1 (H.128)	2 (H.6)	3 (G.101)	4 (G.200)	5 (G.146)	7 (G.99)	8 (G.244)	9 (G.84)
SiO_2	0.06	0.05	0.06	0.10	0.10	0.09	0.07	0.17
TiO_2	48.5	49.2	50.3	49.8	49.4	50.5	49.8	49.5
Al_2O_3	0.13	0.19	0.02	0.07	0.11	0.09	0.09	0.13
V_2O_3	0.58	0.36	0.11	0.10	0.12	0.12	0.06	0.10
FeO	45.9	45.9	47.8	47.2	47.9	47.0	47.4	47.8
MnO	0.35	0.39	0.50	0.47	0.47	0.43	0.53	0.49
MgO	3.64	3.28	0.49	1.17	1.00	1.21	1.28	1.09
CaO	0.16	0.16	0.07	0.27	0.25	0.19	0.11	0.16
Sum	99.3	99.5	99.4	99.2	99.4	99.6	99.3	99.4
				Recalculated analyses				
Fe_2O_3	10.3	8.9	4.4	5.8	6.6	4.8	6.1	6.4
FeO	36.6	37.9	43.8	42.0	42.0	42.7	41.9	42.1
Total	100.3	100.4	99.8	99.8	100.3	100.1	99.9	100.1
Mol. % R_2O_3	10.3	8.9	4.2	5.7	6.5	4.8	5.9	6.3
Temp. °C	775	700	1100	1080	1080	1075	1085	1090
f_{O_2}	$10^{-14.3}$	$10^{-16.4}$	$10^{-10.1}$	$10^{-10.2}$	$10^{-10.1}$	$10^{-10.4}$	$10^{-10.1}$	$10^{-10.0}$

* Below limit of sensitivity 0.02%. ZnO and Cr_2O_3 below limit in all samples except 18 and 25.

[a] Includes 0.04 ZnO.

[b] Includes 0.02 Cr_2O_3.

Mol. % R_2O_3 includes Al_2O_3, Cr_2O_3, V_2O_3 and Fe_2O_3.

puted values for Ca, Mg and Fe derived from analyzed standard pyroxenes of comparable composition were converted to weight percent metasilicate molecules. Normally the sum was between 94 and 96 for an augite and a little higher for a pigeonite or an orthopyroxene; aberrant totals were discarded, and the remaining analyses were recalculated into molecular Ca, Mg and Fe and plotted in Figure 4. The same points of analysis could not subsequently be identified for the analysis of Al, Ti, Mn and Na, but by keeping one spectrometer receiving either Ca or Fe radiation, pyroxenes of comparable type and range of composition were analyzed to give a range of results for each pyroxene type. All the results were averaged in order to arrive at a bulk composition of the two coexisting pyroxene phases; this average may be very far from the true average if the minerals are extensively zoned, but for the purposes of this paper, this method is accounted sufficient.

Only partial analyses were made of the feldspars and olivines again using closely comparable analyzed standards. Chlorophaeite was analyzed using pyroxene standards, and the appropriate corrections for mass absorption and atomic number were made. All determinations of iron are reported as FeO, except for those of chlorophaeite.

MINERALOGY

Iron-titanium oxides. In a general way magnetite (*s.l.*) crystallized late as interstitial ragged grains partially enclosing groundmass plagioclase and pyroxene in the olivine tholeiites (Nos. 1, 2 and 3), whereas in the more iron-rich tholeiites, the order of crystallization has changed and magnetite forms numerous equant evenly distributed crystals precipitating before the groundmass pyroxene and feldspar (Nos. 4, 5, 7, 8, 9, 10). In the basaltic-andesites (Nos. 11, 12 and 13) and the icelandites (Nos. 14, 16 and 17), magnetite is found in two relatively clear-cut size fractions,

TABLE 2—(*Continued*

10 (G.163)	11 (G.194)	12 (G.247)	13 (H.20)	14 (H.107)	16 (G.230)	17 (H.96A)	18 (G.151)	25 (G.94)
0.08	0.12	0.13	0.12	0.06	0.09	0.21	0.05	0.05
49.6	48.8	48.8	48.2	48.1	49.6	49.2	49.8	47.7
0.08	0.06	0.04	0.06	0.11	0.10	0.05	0.04	0.15
0.09	0.03	*	*	*	*	*	*	0.54
47.3	48.9	47.6	49.2	47.8	47.8	48.4	47.7	48.6
0.45	0.59	0.79	0.54	0.64	1.04	0.95	0.98	0.38
1.07	0.54	0.88	1.01	2.24	0.62	0.42	0.62	1.24
0.14	0.16	0.21	0.15	0.06	0.12	0.19	0.06	0.14
98.8	99.2	98.6	99.3	99.0	99.4	99.4	99.3[a]	99.8[b]
				Recalculated analyses—(*Continued*)				
5.7	7.3	6.9	9.2	10.2	6.0	6.5	5.7	9.4
42.2	42.3	41.4	40.9	38.6	42.4	42.5	42.6	40.2
99.4	99.9	99.3	100.2	100.0	100.0	100.0	99.9	99.8
5.6	7.0	6.6	8.8	9.7	5.8	6.2	5.4	9.7
980	840	975	850	950	965	905	925	1050
$10^{-11.6}$	$10^{-13.7}$	$10^{-11.6}$	$10^{-13.2}$	$10^{-11.5}$	$10^{-11.8}$	$10^{-12.7}$	$10^{-12.6}$	$10^{-10.2}$

the larger size fraction being interpreted as microphenocrysts, and the smaller may be considered as part of the quenched groundmass. In the porphyritic pitchstone (No. 18) magnetite is present as microphenocrysts.

Chromite has only been found in an accumulative picrite-basalt (No. 25), in which it occurs as inclusions in the olivine phenocrysts, and also more rarely as independent microphenocrysts mantled by an outer zone of titanomagnetite.

In many of the rocks, the spinel phase has been subsequently oxidized and has unmixed (Buddington and Lindsley 1964) to form either intergrowths of ilmenite and magnetite or compound grains of the two oxide phases. Only in eight rocks are the spinel phases homogeneous and their analyses are given in Table 1. Also shown in Table 1 are the analyses of the oxidized or unmixed spinels together with the analysis of the chromite and its mantle of titanomagnetite.

In all these rocks ilmenite occurs as a discrete phase crystallizing directly from the liquid; exsolution or heterogeneity has not been observed in any ilmenite examined with the microprobe, and their analyses are given in Table 2. No analyses have been made of the ilmenite resulting from oxidation of a spinel phase as their grain size is generally too small. It has also not been possible to analyze the small groundmass spinel phase so characteristic of the basaltic andesites (Nos. 11, 12 and 13) and icelandites (Nos. 14, 16 and 17).

Both sets of analyses of the iron-titanium oxides (Tables 1 and 2) have

been recalculated to check their quality (Carmichael 1967), and as may be seen the totals of the spinel-phases are satisfactory either on the ilmenite basis of calculation or on the ulvospinel basis; the totals of the recalculated ilmenite analyses are also satisfactory. The temperatures ($\pm 30°C$) of the magnetite-ilmenite equilibration are given in Table 2 together with the oxygen fugacities ($10^{\pm 1}$) of their equilibration; these values have been obtained from the curves of Buddington and Lindsley (1964) using a slightly different method for the computation of the molecular percentages of ulvospinel in the spinel-phase, and trivalent ions (R_2O_3) in the ilmenite phase (Carmichael 1967).

The temperatures and oxygen fugacities of the oxide equilibration have been plotted in Figure 1; those rocks with one-phase magnetites have equilibration data which fall near, but below, the curve of the synthetic buffer fayalite-magnetite-quartz.

The extrapolation of this oxide equilibration data to higher temperatures indicates that the derived oxygen fugacities are lower than the range found experimentally by Fudali (1965). This is not surprising as many of the basalts used in Fudali's experiments may have been oxidized subsequently to their crystallization, and consequently the oxygen fugacities required to support these modified ferrous/ferric ratios at 1200°C may not be those of the pristine lavas. Peck and Wright (1966) have directly measured the fugacity of oxygen in the tholeiitic Kilauea lava lakes ($10^{-9.6\pm0.6}$ at 1065°C), the result of which is within the limits of error of those deduced from the one-phase oxide data for the Thingmuli basalts (Table 2).

The oxide equilibration temperatures given in Table 2 for the rocks with one-phase spinels could represent a close approach to the liquidus temperatures of those rocks where magnetite and ilmenite are among the earlier phases to crystallize, namely, the more iron-rich basalts, basaltic-andesites, icelandites and pitchstones. In Figure 2, these oxide equilibration temperatures have been plotted together with the liquidus data for the Hawaiian tholeiitic lavas (Tilley *et al.* 1963). The displacement of these Thingmuli basalts from the Hawaiian liquidus curve is almost within the limits of the oxide technique; the data for the icelandite dyke (No. 16) and the pitchstone dyke (No. 18) fall well below the extension of the Hawaiian curve as may be expected for rocks of such different composition and which may have crystallised in an environment where water vapor pressure could have been considerably greater than 1 atmosphere.

In those rocks with oxidized and unmixed spinel-phases (Table 1), it has been assumed that the ilmenite present in the exsolved or compound grains has the same composition as the discrete ilmenite which precipitated from the silicate liquid. On the basis of this assumption, the

temperatures of the magnetite-ilmenite equilibration and the attendant oxygen fugacities have been given in Table 2 and plotted in Figure 1. These data (Fig. 1) indicate that despite the vagaries in composition of the pervasive steam (groundwater?) which undoubtedly caused much of the oxidation, and which is possibly related to the widespread hydrothermal aureole (Carmichael 1964), the mineralogical assemblages of these rocks have been successful in restricting the oxygen fugacity to the

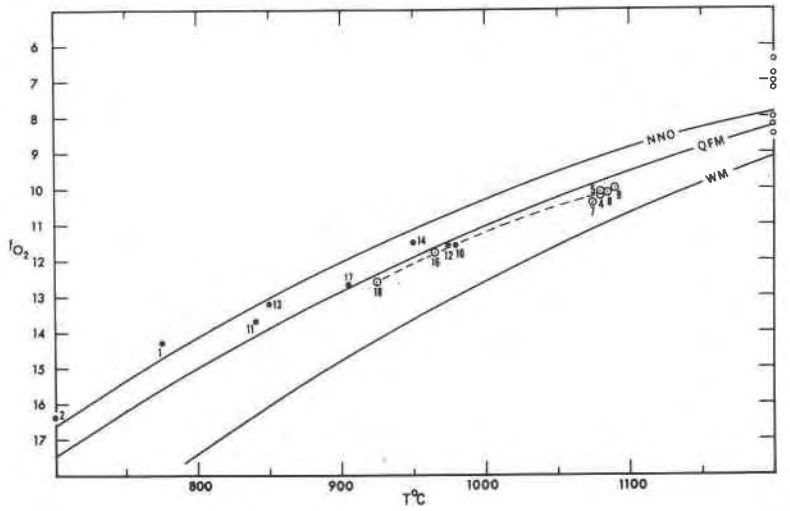

FIG. 1. Values of the temperature and oxygen fugacity ($-\log_{10}$) of the iron-titanium oxide equilibration (Table 2) are plotted; open circles represent one-phase spinel assemblages and filled circles represent unmixed spinel phases. Small open circles at 1200°C are oxygen fugacities of basalts taken from Fudali (1965). The three curves labelled NNO, QFM and WM represent the buffer curves nickel-nickel oxide, quartz-fayalite-magnetite and wustite-magnetite respectively (Eugster and Wones, 1962).

general levels deduced for olivine- or pyroxene-magnetite assemblages (Wones and Eugster 1965; Carmichael 1967).

The variation of the minor elements in the one-phase spinels and the coexisting ilmenites is shown in Figure 3, in which the mineral analyses are plotted against the atomic iron-ratio $Fe^{2+}+Fe^{3+}+Mn/Fe^{2+}+Fe^{3+}+Mn+Mg$ of the host rock (Carmichael 1964); this function progressively increases from the relatively basic olivine-tholeiites to the porphyritic pitchstone. It may be seen (Fig. 3) that as this function of the host rock increases, the contained ilmenites become impoverished in MgO, Al_2O_3 and V_2O_3, in a similar way to those of the Skaergaard intrusion (Vincent and Phillips 1954). The one-phase magnetites show a less pronounced diminution of MgO and V_2O_3 and become slightly enriched in

ZnO in the more acid rocks; as is to be expected MnO increases in both oxide minerals as the iron-function increases. CaO and SiO_2 are present in small amounts in both oxide minerals, SiO_2 being characteristically higher in the spinel phase.

The general conclusion from the one-phase spinel-ilmenite equilibration data is that there is a smooth and progressive decrease in oxygen

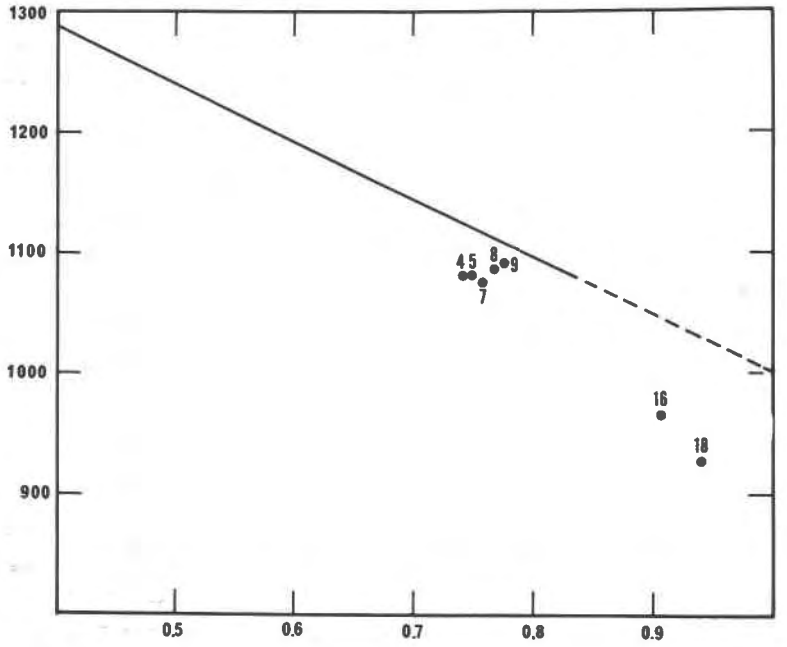

FIG. 2. The iron-titanium oxide equibration temperatures for the one-phase spinels, which are considered to represent the liquidus of the host rocks, plotted against the weight ratio $FeO+Fe_2O_3/FeO+Fe_2O_3+MgO$ of the rocks. The line represents the liquidus data at 1 atmosphere of the Hawaiian tholeiitic series (Tilley et al. 1963).

fugacity throughout the Thingmuli series (Fig. 1), the values of which are essentially those of the synthetic fayalite-magnetite-quartz buffer at the appropriate temperature. Osborn (1959) has suggested that the Skaergaard intrusion and nonorogenic tholeiitic liquids which show a similar absolute enrichment in iron have fractionated with a low fixed-oxygen content; if the evidence of this course of fractionation is endowed to the volcanic products, then the data of the Thingmuli series are in accord with Osborn's hypothesis (Carmichael 1964). However, as it is difficult to conceive of an erupting volcano with a fixed-oxygen content, the emphasis should probably be placed on the buffer capacity of the silicate

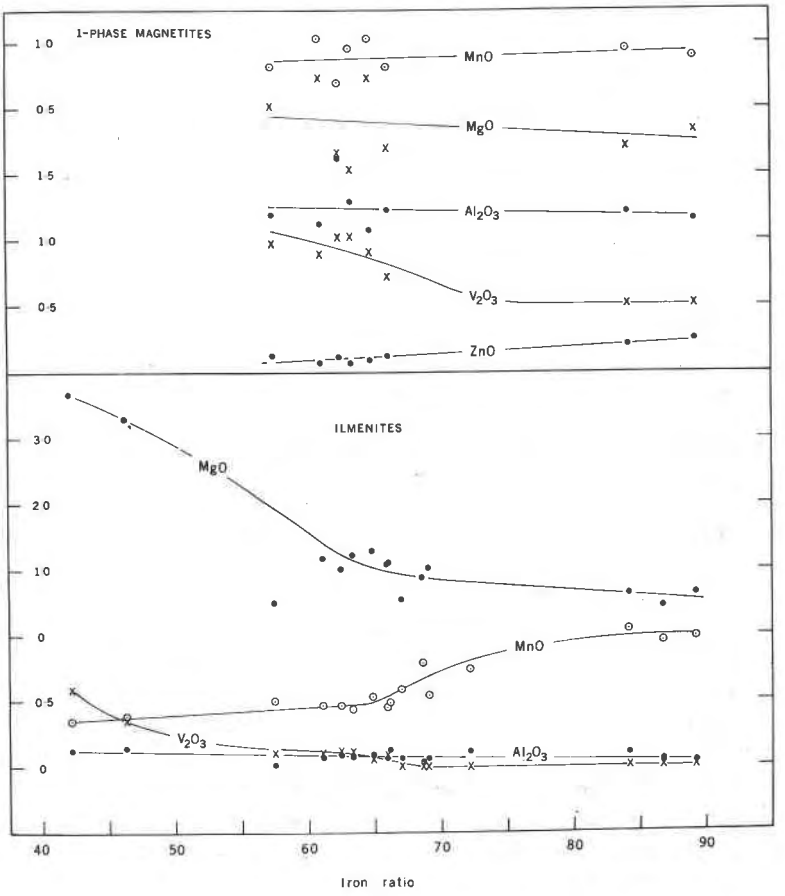

FIG. 3. Variation in weight percent of the minor elements of the one-phase magnetites (Table 1) and ilmenites (Table 2) plotted against the atom ratio $Fe^{2+}+Fe^{3+}+Mn\times100/Fe^{2+}+Fe^{3+}+Mn+Mg$ (iron-ratio) of the host rock (Carmichael (1964). As five one-phase magnetite grains have been found in No. 3 (Table 1), their data has been plotted here.

liquid-solid assemblages, which from the data of Figure 1, was not overwhelmed by a volatile phase of variable composition.

The temperatures deduced from the oxide-equilibration data may represent a close approach to the liquidus temperatures of many of the basaltic lavas; values of approximately 1080°C seem not inconsistent with the available liquidus data on basaltic rocks.

Pyroxenes. When the basalts and basaltic-andesites were examined optically (Carmichael 1964), it was noted that the augite in the groundmass frequently had an outer zone of uniaxial pyroxene considered to be

pigeonite. This characteristic tholeiitic assemblage was identified in all those rocks which are coarse-grained enough for optical determination. It was considered that this pyroxene texture represented augite zoned continuously to pigeonite, but it also possibly represents augite mantled by pigeonite with a compositional break between them. The technique used to discriminate between these two possibilities has been described above, and the evidence of the microprobe analyses indicates that there are two distinct pyroxene species in the groundmass of the picrite-basalt, the basalts and the basaltic-andesites, with a well-defined miscibility gap between them.

The analyses of the pyroxenes, whether groundmass or phenocryst, have been plotted in Figure 4, and a compilation of all the analyses is given in Figure 5a. The groundmass pigeonites present in the picrite-basalt (No. 25), in the basalts and basaltic-andesites (Nos. 1 to 13) show a small but steady increase in Ca as they become enriched in Fe similar to the trend found by McDougall (1961) for the pigeonites of the Red Hills dolerite-granophyre sequence. By contrast, the augites tend to show a decrease in Ca as Fe replaces Mg, the tendency being more marked in the olivine-tholeiites (Nos. 1 and 2) whose augites show less variability in Ca than those of the more iron-rich tholeiites (Nos. 5 to 13) and basaltic-andesites.

In three basaltic rocks, no evidence of a calcium-poor groundmass pyroxene has been found with the electron-probe; however in one of these (No. 5) the place of pigeonite (orthopyroxene has never been identified in the basalts and basaltic-andesites) is presumably taken by an iron-rich olivine in the groundmass. In the other two rocks (Nos. 3 and 4) pigeonite has been rarely identified optically and it must be present only in very small amounts.

The average analyses of the coexisting groundmass pyroxenes are given in Table 3, and their formulae are given in Table 6[1]; these latter data may be used to support the worth of the analytical technique, there being a satisfactory cation distribution if silica is assumed to represent the balance of the analyses of Table 3. Although these averages are unlikely to represent closely the bulk composition of each of the groundmass pyroxene phases, the discrepancy is not of importance here, as the averages are only used to represent a trend of the groundmass pyroxenes and of their tie-lines.

Only the pyroxene phenocrysts of the icelandites (Nos. 14, 16 and 17)

[1] Table 6, calculating formulae of pyroxenes, and Table 7, containing analyses of feldspars, have been deposited as Document 9658 with the American Documentation Institute, Photoduplication Service, Library of Congress, Washington, D. C. 20540. Copies may be secured by citing the document number and remitting in advance $1.25 for photoprints or $1.25 for microfilm.

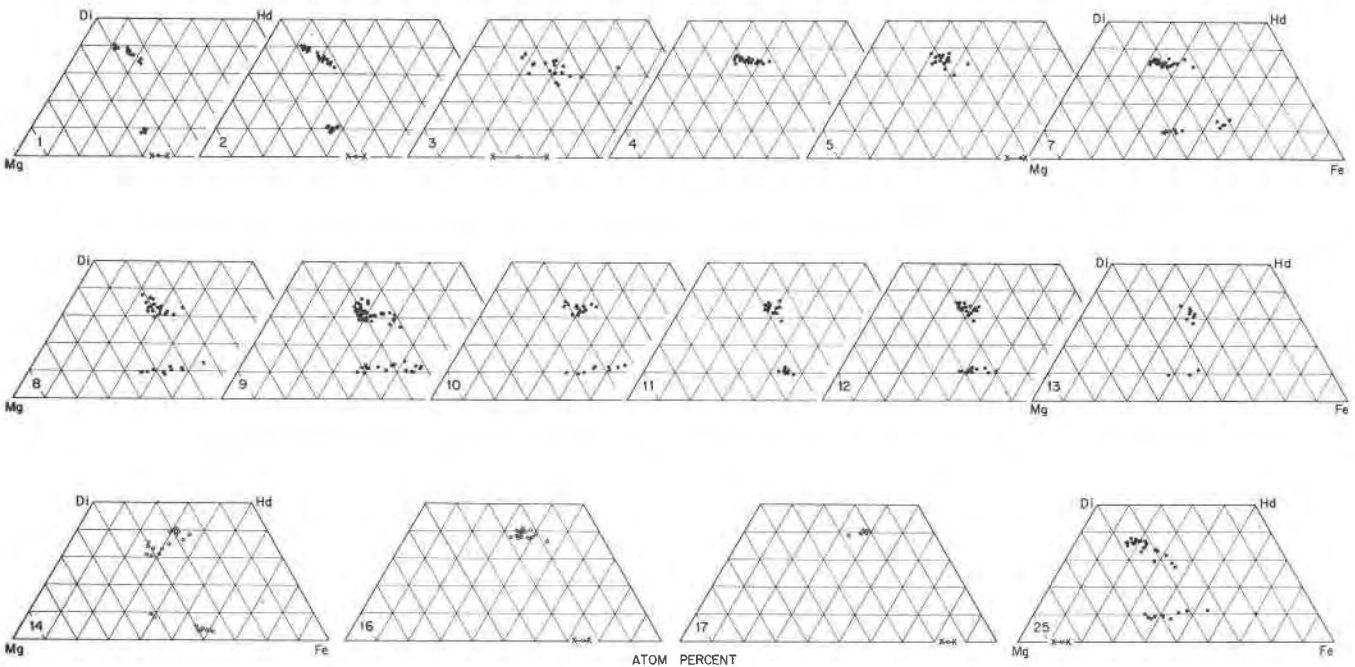

FIG. 4. Variation in the components Ca, Mg and Fe of the pyroxenes recalculated to a molecular basis. The range of zoning (crosses) and average composition of the associated olivines (Table 4) are plotted on the base. Filled circles represent groundmass constituents and open circles represent phenocrysts.

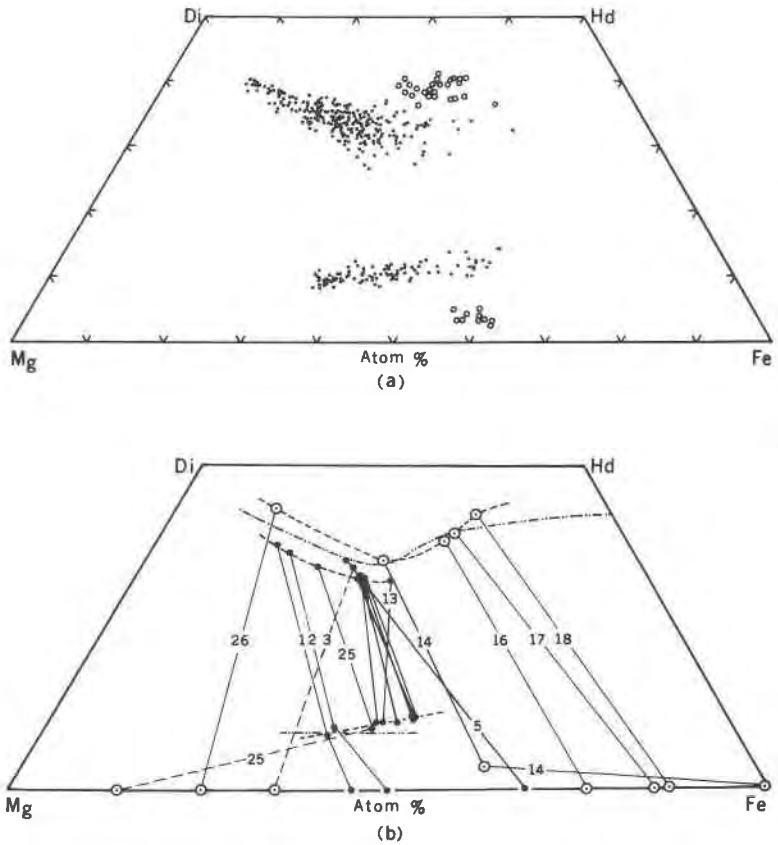

FIG. 5. *a*. Compilation of the data shown for individual rocks in Fig. 4 is plotted here with phenocrysts represented by open circles. Some of the phenocryst data for No. 14 (Fig. 4) have been omitted for clarity.

b. The average analyses of the pyroxenes (Table 3) plotted in terms of Ca, Mg and Fe+Mn. The average analyses of olivines are also plotted on the base (Table 4). Filled circles represent groundmass constituents and open circles represent phenocrysts. Coexisting phenocryst and coexisting groundmass assemblages are joined by continuous tie-lines; dashed tie-lines connect associated phenocryst-groundmass assemblages. The data for 18 and 26 are taken from Carmichael (1960) and (1964) respectively. The dash-double-dot line represents the Skaergaard trend. The Thingmuli phenocryst and groundmass pyroxene trends are indicated by dashed lines.

have been analyzed as the groundmass pyroxenes are too small for the electron-probe; unlike the basalts and basaltic andesites, pyroxene phenocrysts are common in the icelandites. In No. 14, a phenocryst assemblage of pigeonite, orthopyroxene, fayalite, and of an augite of considerable compositional variation, suggests that some of these phases are xeno-

TABLE 3. ANALYSES OF PYROXENES: MEAN OF VALUES PLOTTED IN FIGURE 4 (A, CALCIUM-RICH PYROXENE: B, CALCIUM-POOR PYROXENE: C, ORTHOPYROXENE)

	1(H.128)		2(H.6)		3(G.101)	4(G.200)	5(G.146)	7(G.99)		8(G.244)	
	1A	1B	2A	2B	3A	4A	5A	7A	7B	8A	8B
TiO_2	0.97	0.58	1.10	0.59	1.04	1.17	1.25	0.94	0.56	1.07	0.56
Al_2O_3	1.77	0.68	1.78	0.61	1.54	1.84	1.70	1.31	0.52	1.38	0.59
FeO	9.8	22.9	11.1	22.7	17.6	15.3	15.3	16.6	27.6	17.2	25.0
MnO	0.19	0.46	0.22	0.51	0.37	0.30	0.30	0.31	0.53	0.43	0.60
MgO	16.2	19.2	15.7	18.4	12.7	13.0	13.1	13.0	14.0	12.9	15.8
CaO	18.4	4.3	17.8	4.8	15.3	16.5	16.5	16.2	5.3	15.3	4.9
Na_2O	0.32	0.11	0.33	0.12	0.25	0.29	0.34	0.26	0.09	0.22	0.09
Atom percent											
Ca	37.8	8.7	36.7	9.9	32.6	35.3	35.2	34.1	11.3	32.5	10.4
Mg	46.2	54.2	45.1	52.7	37.6	38.7	38.8	38.1	41.7	38.2	46.9
Fe+Mn	16.0	37.1	18.2	37.4	29.8	26.0	26.0	27.8	47.0	29.3	42.7
Range in concentration in calcium-rich pyroxenes (weight percent)											
TiO_2	1.27–		1.51–		1.56–	1.38–	1.54–	1.16–		1.18–	
	0.79		0.96		0.68	1.02	0.76	0.79		0.95	
Al_2O_3	2.46–		2.21–		2.18–	2.54–	2.33–	1.69–		1.51–	
	0.83		1.03		0.94	1.46	1.14	0.90		1.26	
MnO	0.13–		0.16–		0.20–			0.26–		0.37–	
	0.29		0.30		0.66			0.54		0.61	

	9(G.84)		10(G.163)		11(G.194)		12(G.247)		13(H.20)	
	9A	9B	10A	10B	11A	11B	12A	12B	13A	13B
TiO_2	1.04	0.65	1.10	0.65	0.95	0.57	0.95	0.69	—	—
Al_2O_3	1.20	0.72	1.31	0.72	1.14	0.59	1.16	0.72	—	—
FeO	18.3	27.8	17.4	27.2	17.2	26.6	17.2	25.6	20.0	26.1
MnO	0.42	0.61	0.38	0.60	0.48	0.75	0.51	0.73	—	—
MgO	13.1	13.9	12.5	13.8	12.8	14.8	12.8	15.5	11.4	15.5
CaO	14.8	5.4	15.2	5.0	15.6	4.8	15.6	5.0	14.9	4.7
Na_2O	0.24	0.10	0.27	0.08	0.31	0.11	0.28	0.11	—	—
Atom percent										
Ca	30.7	11.5	32.7	10.9	33.1	10.3	33.0	10.6	32.2	10.1
Mg	38.2	41.2	37.4	41.8	37.7	44.0	37.7	45.8	34.2	46.2
Fe+Mn	31.1	47.3	29.9	47.3	29.2	45.7	29.3	43.6	33.6	43.7
Range in concentration in calcium-rich pyroxenes (weight percent)										
TiO_2	1.20–		1.53–		1.60–		1.12–			
	0.74		0.93		0.63		0.84			
Al_2O_3	1.42–		1.77–		1.36–		1.28–			
	0.97		0.91		0.91		1.02			
MnO	0.37–		0.34–				0.41–			
	0.52		0.49				0.66			

	14(H.107)			16(G.230)	17(H.96A)	18(G.151)	25(G.94)		26(H.92)
	14A phenocrysts	14B phenocrysts	14C phenocrysts	16A phenocrysts	17A phenocrysts	18A[a] phenocrysts	25A	25B	26A[b] phenocrysts
TiO_2	0.97	0.55	0.20	1.12	0.98	0.47	1.09	0.68	0.90
Al_2O_3	2.36	1.08	0.34	1.88	1.93	0.99	1.74	0.67	3.08
FeO	18.0	24.4	34.4	21.3	21.2	22.45	13.6	25.3	7.94
MnO	0.62	0.94	1.06	0.70	0.66	0.73	0.29	0.43	0.17
MgO	11.4	17.8	12.0	7.9	7.2	5.93	14.5	16.1	15.29
CaO	16.6	4.3	1.7	17.4	17.6	19.47	16.2	4.5	20.97
Na_2O	0.26	0.13	0.04	0.26	0.30	0.66	0.23	0.11	0.46
Atom percent									
Ca	35.3	8.8	3.7	38.2	39.4	42.5	34.3	9.6	43.2
Mg	33.7	50.7	36.2	24.1	22.4	18.0	42.7	47.7	43.8
Fe+Mn	31.0	40.5	60.1	37.7	38.2	39.5	23.0	42.7	13.0
Range in concentration in calcium-rich pyroxenes (weight percent)									
TiO_2	1.74–			1.38–	1.31–		1.53–		
	0.55			0.68	0.57		0.80		
Al_2O_3	2.82–			2.51–	2.70–		3.15–		
	1.23			1.02	1 10		1.09		
MnO	—			0.63–	0.58		0.19–		
				0.79–	0.77		0.47		

[a] Analysis No. 6, Table 2, Carmichael (1960). Fe_2O_3 recalculated to FeO.
[b] Analysis No. 26 Px, Table 7, Carmichael (1964). Fe_2O_3 recalculated to FeO.

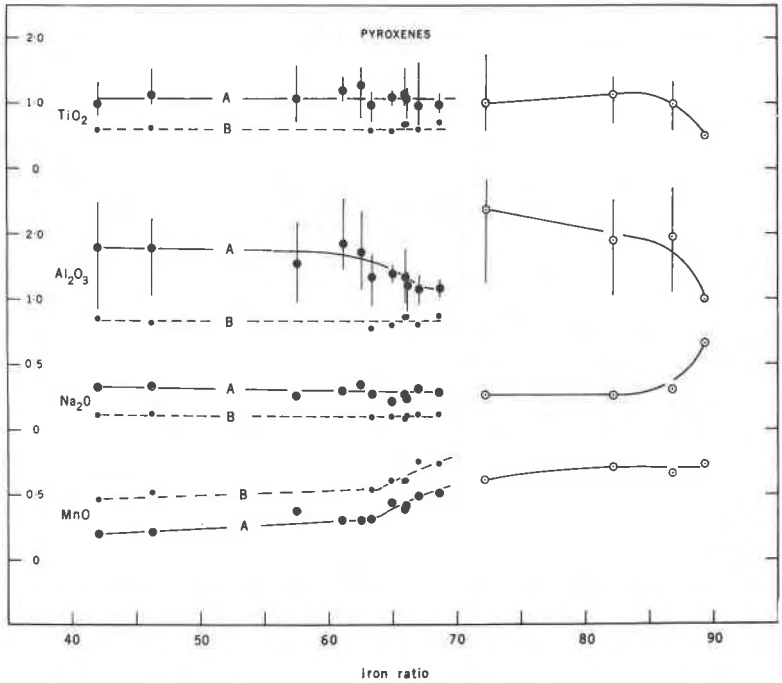

FIG. 6. Variation in weight percent of the minor elements in the average analyses of the pyroxenes (Table 3) plotted against the atom ratio $Fe^{2+}+Fe^{3+}+Mn\times100/Fe^{2+}+Fe^{3+}+Mn+Mg$ of the host rocks (Carmichael 1964). A represents the calcium-rich pyroxenes and B represents the pigeonites. Filled circles are groundmass constituents and open circles are phenocrysts. The length of the vertical line represents the range of variation of the element (Table 3).

crysts. The petrographic evidence is not decisive, but probably the pigeonite and the more magnesian augites are foreign; whether or not the fayalite phenocrysts are xenocrysts is less clear optically, but their composition appears too extreme to be in equilibrium with the orthopyroxene. In the other two icelandites (Nos. 16 and 17), only a calcium-rich pyroxene is present as a phenocryst, together with an iron-rich olivine (Fig. 5b).

The distribution of the minor elements between the coexisting groundmass pyroxenes follows the familiar pattern of those of the Skaergaard intrusion (Brown 1957). Augite is always enriched in Al_2O_3, TiO_2 and Na_2O with respect to the coexisting pigeonite (Fig. 6) and impoverished in MnO; the pigeonites typically contain little or no Al_2O_3 in tetrahedral coordination, a feature also found in the icelandite orthopyroxene phenocrysts (No. 14). Both groundmass pyroxenes are zoned with respect to the minor elements as well as the major elements; in all the groundmass

augites Al_2O_3 decreases and MnO increases as the pyroxene becomes enriched in iron (Table 3); TiO_2 shows a more irregular relationship with respect to the increase in iron in the augites, but it also tends to decrease. The ranges of values of Al_2O_3, TiO_2 and MnO for the pigeonites are not given in Table 3 as apart from MnO, the variation of Al_2O_3 and TiO_2 usually lies within the error of the analytical technique.

The variation of the minor elements in both the groundmass and phenocryst pyroxenes is shown in Figure 6 as a function of the iron-ratio (Carmichael 1964) of the rock which contains them. There is a tendency for the average value of Al_2O_3, and its range of variability, to decrease in the groundmass augites as the iron-ratio of the rock increases. The augite phenocrysts of the icelandites do not lie on the continuation of the groundmass augite trend with respect to Al_2O_3 (Fig. 6), a feature also evident in terms of Ca, Mg and Fe (Fig. 5). Na_2O shows little variation in the pyroxenes as a whole, although it increases in the chrome-bearing diopsidic augite (Table 3, No. 26; Fig. 5b) at one extreme, and in the ferroaugite phenocrysts of the pitchstone at the other (Table 3, No. 18). MnO rises continuously in all pyroxenes as the iron-ratio of the rock increases (Fig. 6), and has the same curious step in its variation curve as the MnO curve of ilmenite (Fig. 3).

The crystallization of pyroxene in volcanic rocks. The pyroxene trends of the large slowly cooled tholeiitic intrusives, of which the Skaergaard is one example, has established a well-defined miscibility gap (two-pyroxene field) between coexisting calcium-rich pyroxenes and calcium-poor pyroxenes (Brown 1957). This gap, which is caused by the intersection of the crystallization surface with the pyroxene solvus, is wider for the coexisting pyroxene phenocrysts of acid rocks, where the augite tends to be more calcium-rich and the orthopyroxene more calcium-poor, than the comparable phases in basic rocks (Carmichael 1967). It has been suggested earlier that this extension of the width of the miscibility gap is the result of the depression of the crystallization surface in in acid rocks with respect to the pyroxene solvus (Carmichael 1963b), but new data on the temperatures of crystallization of both basaltic and acid liquids may indicate that the explanation is not so simple as this.

The groundmass pyroxenes of many Hawaiian tholeiitic lavas (Muir and Tilley 1964) and Japanese lavas (Kuno 1955) have compositions which fall in the miscibility gap, and represent a progressive variation trend of augite through subcalcic augite to pigeonite. This pyroxene trend, namely, the predominant substitution of Fe^{2+} for Ca^{2+} in the pyroxene structure, has been suggested by Muir and Tilley (1964) to be representative of the crystallization of basaltic magma under effusive

conditions, and, as many of these pyroxenes are metastable (Yoder *et al.* 1963), has been christened the metastable or quench trend.

The presence of two coexisting pyroxene phases in the groundmass of the Thingmuli basalts and basaltic-andesites (most of which are lavas, Table 1) and also in a basalt of the Hawaiian Koolau series (Muir and Long 1965) indicates that a metastable subcalcic augite is not invariably present. Moreover, the similarity of trend of the tie-lines joining coexisting groundmass pyroxenes in the Thingmuli basaltic rocks (Fig. 5b) with those of the Skaergaard (Brown 1957; Brown and Vincent 1963) suggests that, insofar as the average compositions of these pyroxenes are representative (Table 3), the two phases are in equilibrium one with the other. Thus the distinction made by Muir and Tilley (1964) between the metastable or quench pyroxene trend of the volcanic effusives on the one hand, and the intratelluric or equilibrium trend on the other (e.g. Skaergaard) cannot be related solely to the rate of cooling, and the term "quench" in this context is possibly best forgotten.

The writer can see no obvious reason why one set of tholeiitic lavas (Hawaiian) should typically have a metastable groundmass pyroxene, whereas another tholeiitic lava series (Thingmuli) should have groundmass pyroxenes which match in their variation trends, although with a distinctly narrower miscibility gap (Fig. 5b), the pyroxenes of the slowly cooled intrusions. The only major compositional difference between these two suites is the iron-rich nature of the Icelandic series which, by decreasing the viscosity and temperature of the liquids, could perhaps encourage an equilibrium assemblage. There are not yet sufficient data on the Hawaiian tholeiitic groundmass pyroxenes to indicate the extent of their zoning in terms of iron-enrichment (*cf.* however Muir and Long 1965) to show whether or not they are also more magnesian than the Thingmuli pyroxenes.

The analogy between the coexisting pyroxenes of the Thingmuli basalts and basaltic-andesites and those of the Skaergaard intrusion, may, with some liberty, be extended further. The occurrence of olivine in the groundmass of the olivine-tholeiites (Nos. 1 and 2) and in one of the basalts (No. 5; Figs. 4 and 5) is of contrasted character. In the olivine-tholeiites, olivine and a pigeonite with a restricted range of zoning coexist (Fig. 4), and the trend of their tie-lines (Fig. 5b) is not dissimilar to the olivine-inverted pigeonite tie-lines of the Skaergaard lower gabbros. In the ferrogabbros of the Skaergaard upper zone, an iron-rich olivine reappears as a cumulus phase, co-precipitating with an iron-rich pigeonite which, after a short interval, ceases to crystallize, and therefore defines the limit of the two-pyroxene field. If it may be assumed that the composition in terms of the iron/magnesium ratio of the groundmass pyro-

xene components of the Thingmuli basalts and basaltic-andesites is controlled by the extent of the prior crystallization of the iron-titanium oxides, then there will be no simple relationship between the Fe/Mg ratio of the rock as a whole and that of the groundmass pyroxenes. It may be suggested, therefore, that with respect to the crystallization of the pyroxene-olivine groundmass phases, the olivine-tholeiites represent the stage of the Skaergaard lower gabbros, and with one exception, the remaining basalts and basaltic-andesites represent the state of the olivine-free middle gabbros. The sole exception (No. 5), which contains an iron-rich olivine rather than pigeonite, is a possible representative of the state where the Skaergaard ferrogabbros have just passed through the limit of the two-pyroxene field. This analogy would be more convincing if the augite in No. 5 was demonstrably more iron-rich than the augites of those rocks which also contain pigeonite; unfortunately this is not the case (Fig. 4) so the presence of an iron-rich olivine rather than pigeonite in the groundmass of No. 5 remains an enigma.

The cessation of crystallization of a calcium-poor pyroxene, or the limit of the two-pyroxene field, in basaltic magma has received much attention in the literature, the various hypotheses having been reviewed by Brown (1957) and Yoder *et al.* (1963). In the basalt No. 5 discussed above, an iron-rich olivine apparently takes the place of pigeonite with no petrographic evidence of the nature of the mutual relationship between the two possible phases. In the icelandites, one of which contains phenocrysts of orthopyroxene, there is also no indication of the relationship between this phase and olivine which is presumably its substitute as a phenocryst in the other icelandites and the porphyritic pitchstone (Fig. 5b). The Thingmuli series offers no new evidence on the nature of the actual relationships between olivine and a calcium-poor pyroxene at the limit of the two-pyroxene field; the two phases are antipathetic, suggestive of the reaction relationship postulated by Poldervaart and Hess (1951, p. 479).

The evidence of the slowly cooled tholeiitic intrusives (Brown 1957; Hess 1941) indicates that an orthorhombic pyroxene is the low temperature stable equivalent of a higher-temperature calcium-poor monoclinic pyroxene (pigeonite). Kuno (1966) has made a spirited attempt to reconcile this evidence from natural assemblages with the new, apparently conflicting, experimental evidence on the pyroxenes (Boyd and Schairer 1964; Boyd and England 1965; Lindsley 1965). If pigeonite and orthopyroxene are simply related one to the other by a temperature-dependent inversion curve (Bowen and Schairer 1935), then it is surprising that the groundmass pyroxene assemblages of the basalts and basaltic-andesites never include an orthopyroxene, indicating that their crystalliza-

tion curve never intersected the orthopyroxene field. By contrast, orthopyroxene is a typical calcium-poor pyroxene phenocryst in one of the icelandites (No. 14) and is also found as a common phenocryst in a wide variety of acid rocks (Carmichael 1967); the total range of composition of these orthopyroxenes in terms of their iron/magnesium ratios shows a complete overlap with the pigeonitic pyroxenes in the Thingmuli basalts and basaltic-andesites. The conventional explanation is presumably that the crystallization temperatures of the phenocrysts in the icelandite and the acid rocks is lower than that of the groundmasses of the basalts, and certainly this hypothesis would tend to be supported by the more calcic augites of the acid rocks (Fig. 5; Carmichael 1967), but to the writer, it is doubtful whether this postulate can be sustained, and it is likely that there is (or there will be shown to be) some overlap in the temperatures of crystallization of the two groups of rocks. This, at present an unsupported conjecture, implies that the bulk composition of the system in which the pyroxenes are precepitating, and the nature of the other phases, will have some influence on their species and composition.

Olivine. Olivine occurs as phenocrysts and as a groundmass constituent in the Thingmuli series, although it has not been found in both roles in the same rock. It is most abundant in the accumulative picrite-basalt No. 25 which contains large phenocrysts of magnesian olivine, and it is an essential constituent of the olivine-tholeiite lavas (Nos. 1 and 2) where it is found in the groundmass. In the relatively coarse-grained olivine-dolerite dyke (No. 3), zoned olivine phenocrysts are common, and in the icelandites and pitchstone, an iron-rich olivine is a characteristic phenocryst phase.

The analyses of the olivines are given in Table 4, and represent the averages of between ten and twenty olivine crystals in each rock except from the icelandite No. 14 in which only two crystals have been found. These averages have been recalculated into the various olivine molecules and their summation indicates that the analyses are satisfactory. Zoning is present in most of the analyzed olivines, and its range in terms of weight percent of the forsterite molecule is also given in Table 4; there is no clear relationship between the extent of the zoning and the presence of olivine as either a phenocryst or a groundmass constituent. It may be seen from the data in Table 4 that CaO and MnO increase concomitantly with iron in the olivines; CaO is always above the level of 0.14 weight percent which Simkin and Smith (1966) consider separates plutonic olivines from those which have crystallized in a volcanic environment.

The average composition of each of the olivines and their range of zoning have been plotted in Figure 4, and in Figure 5b the relationship

TABLE 4. ANALYSES OF OLIVINES

	1(H.128)	2(H.6)	3(G.101)	5(G.146)	14(G.107)	16(G.230)	17(H.96A)	18(G.151)[a]	25(G.94)[b]
			phenocrysts		phenocrysts	phenocrysts	phenocrysts	phenocrysts	phenocrysts
FeO	37.6	40.7	29.9	51.8	67.5	55.4	60.0	62.24	11.97
MnO	0.48	0.56	0.38	0.69	1.96	1.77	1.91	1.24	0.19
MgO	26.2	23.6	32.1	14.2	0.21	10.3	6.3	5.34	47.03
CaO	0.36	0.33	0.28	0.56	0.39	0.65	0.45	0.49	0.24
NiO	—	—	—	—	—	—	—	—	0.26
				Recalculated analyses (weight percent)					
Fa	53.3	57.7	42.4	73.4	95.7	78.6	85.1	88.2	17.0
Tp	0.7	0.8	0.5	1.0	2.8	2.5	2.7	1.8	0.3
Fo	45.7	41.2	56.0	24.8	0.4	18.0	11.0	9.3	82.1
La	0.6	0.5	0.4	0.9	0.6	1.0	0.7	0.7	0.4
Total	100.3	100.2	99.3	100.1	99.5	100.1	99.5	100.0	100.2[c]
Variation in Fo component; weight percent									
	48.3–42.9	45.9–38.2	64.7–40.1	34.9–17.1	—	20.4–12.6	13.1–8.7	—	83.2–74.2
Molecular ratio (Fe+Mn) 100/Fe+Mn+Mg									
	44.9	49.5	34.6	67.5	99.5	75.7	84.6	87.0	12.7

[a] Analysis No. 6B, Table 4, Carmichael (1960). Fe_2O_3 recalculated to FeO.

[b] Analysis 250L, Table 7, Carmichael (1964). Fe_2O_3 recalculated to FeO.

[c] Includes 0.4 Ni_2SiO_4.

of the olivines to their coexisting pyroxenes may be seen. For those rocks in which the olivine-pyroxene assemblages are solely groundmass constituents (Nos. 1, 2 and 5; Fig. 5b) and for those in which they are phenocryst assemblages (Nos. 14, 16, 17, 18 and 26), the comparison of the trend of their tie-lines with the equivalent equilibrium assemblages of the Skaergaard intrusion is surprisingly close and indicates equilibrium assemblages in both groups of rocks. As is to be expected from the data on the system MgO-FeO-SiO_2 (Bowen and Schairer 1935), the olivines are more enriched in iron than their associated pyroxenes.

The rather unusual occurrence of an olivine in the groundmass of a basalt (No. 5, Figs. 4 and 5b) in place of a pigeonite has been discussed above; as may be seen in Fig. 4, this groundmass olivine is more iron-rich than almost all the iron-rich zones of pigeonite found in this series, and is possibly a natural representative of the reaction-relation of an iron-rich calcium-poor pyroxene with liquid (Bowen and Schairer 1935). It is unlikely that the two almost pure fayalite phenocrysts in the icelandite No. 14 (Fig. 5b) also represent this relationship as they appear far too extreme in composition to be associated in this way with the coexisting orthopyroxene; accordingly they may be accounted xenocrysts.

In the accumulative picrite-basalt (No. 25) and the olivine-dolerite dyke (No. 3), the tie-lines (Fig. 5b) joining the phenocrysts to the groundmass pyroxenes are aberrant in trend; this is to be expected for any phenocryst-groundmass relationship. If the groundmass pyroxenes represent the quenched product of the liquid in equilibrium with the phenocrysts, then "aberrant" tie-lines are no certain indication of dis-equilibrium.

In the account of the petrology of the Thingmuli series (Carmichael 1964), it was shown that there was a stage in the liquid line of descent of this series where olivine was not precipitated. Thus the presence of olivine in the olivine-tholeiites (Nos. 1 and 2), its absence in the basalts and basaltic-andesites (see page 1831 however) and its reappearance as an iron-rich phenocryst phase in the icelandites and pitchstones suggest a recurrence analogous to that of olivine in the Skaergaard intrusion (Wager and Deer 1939); this intrusion in turn may be a more complex natural equivalent of fractionation in the system MgO-FeO-SiO_2 (Bowen and Schairer 1935) in which the recurrent crystallization of olivine is also found. In the Thingmuli series, this simplified analogy has been complicated by the precipitation of microphenocrysts of a spinel-phase more or less at the stage at which olivine disappears; the inclusion of magnetite in the fractionated crystalline assemblage is believed to have caused the rather curious halt in the otherwise progressive increase in the iron-ratio of the series (Carmichael 1964).

Plagioclase. Plagioclase is the only feldspar found either as a phenocryst or as a predominant groundmass constitutent in the Thingmuli series; scattered plagioclase phenocrysts in varying amounts are present in all the rocks, but only in the olivine-dolerite dyke (No. 3) are the plagioclase glomeroporphyritic clusters possible cognate xenocrysts.

As all the feldspars examined are zoned, the bulk composition of the plagioclase, whether as phenocrysts or in the groundmass, is not easy to determine, and would presumably require the analysis of numerous crystals from core to margin. Approximately twenty crystals in each rock have been analyzed with the microprobe, the directly determined values of Na, K and Ca having been recalculated to weight percent equivalent feldspar molecules and plotted in Figure 7. The average values for the

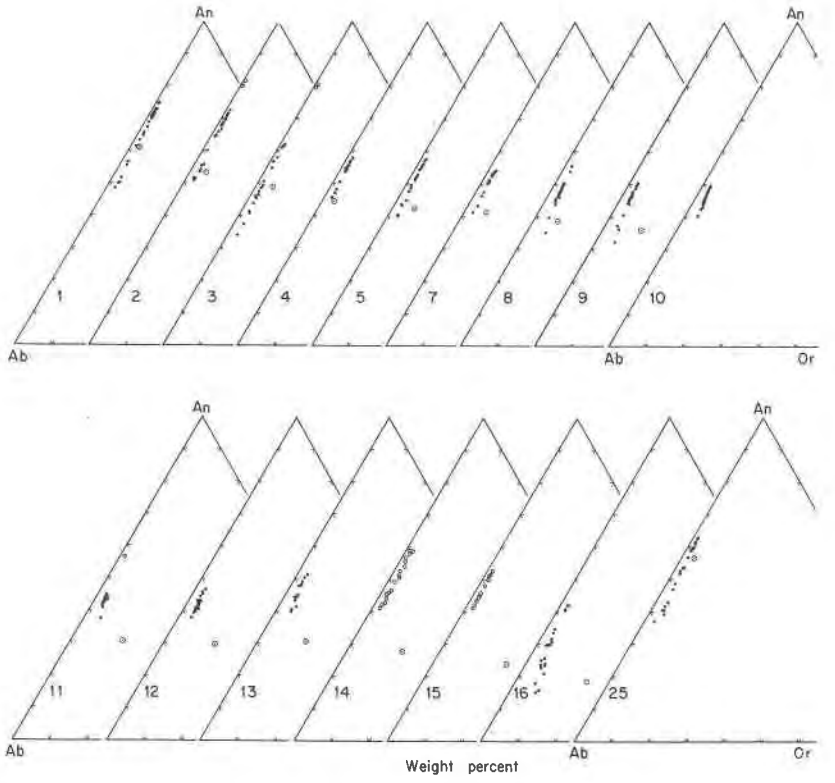

FIG. 7. The variation in composition of the plagioclase feldspars represented in terms of three components albite (Ab), potassium feldspar (Or) and anorthite (An). Groundmass constituents are represented by filled circles, phenocrysts by open circles, and the normative feldspar of each rock by a large open circle.

plagioclase in each rock are given in Table 7[1], together with the most extreme values (Ab-rich and An-rich) found; this range may be taken to approximate to the extent of the zoning. The totals of the analyses (Table 7) when recalculated to weight percent feldspar molecules are generally low; this may in part be due to the presence of undetermined Sr and Ba, but is more likely to reflect the now rather dated technique for the determination of Na with the electron-probe.

The plagioclase phenocrysts in the olivine-tholeiites (Nos. 2 and 3) are similar in composition to those phenocrysts found in accumulative rocks and analyzed by wet chemistry (Carmichael 1964, No. 26); their outer rims correspond in composition with their associated groundmass feldspars.

In the sequence olivine-tholeiite to basaltic-andesite (Fig. 7, Nos. 1–13), the groundmass plagioclase becomes progressively more sodic, and the range of composition, or zoning, becomes more restricted. Thus in the olivine-tholeiites (Nos. 1–3) and the picrite-basalt (No. 25), the zoning extends over a range of about twenty percent of anorthite, whereas in the basaltic-andesites (Nos. 11 to 13) it is restricted to perhaps ten percent anorthite. The normative feldspar for each of these rocks is invariably more potassic than the modal feldspar, and is frequently more sodic as well (Fig. 7, Table 7). This progressive restriction in the extent of the zoning of the groundmass plagioclase is no doubt a reflection of the increase in amount of the glassy residuum (Hoffer 1966) or its chloritic alteration product.

In the icelandites and pitchstones, the groundmass feldspar is either too small to be determined with the electron-probe, or it is occult in an interstitial glassy groundmass. The plagioclase phenocrysts in the icelandites are also zoned over a range of approximately ten percent anorthite, but in one icelandite (No. 16) the small phenocrysts show every gradation in size down to large microlites, and are more extensively zoned (Fig. 7).

The data in Figure 7 show that there is an increasing discrepancy as the rocks become more silicic between the composition of the modal feldspar and that of the normative feldspar. Although it is doubtful if the composition of the normative feldspar represents a very close approach to the composition of a modal feldspar which would result from crystallization under equilibrium conditions, the discrepancy, following the time honored custom of ignoring what cannot be treated (Bottinga *et al.* 1966), is taken to be trivial. Thus it is assumed that the normative feldspar in each rock (Fig. 7) is a composition which could be achieved by

[1] See footnote on page 1824.

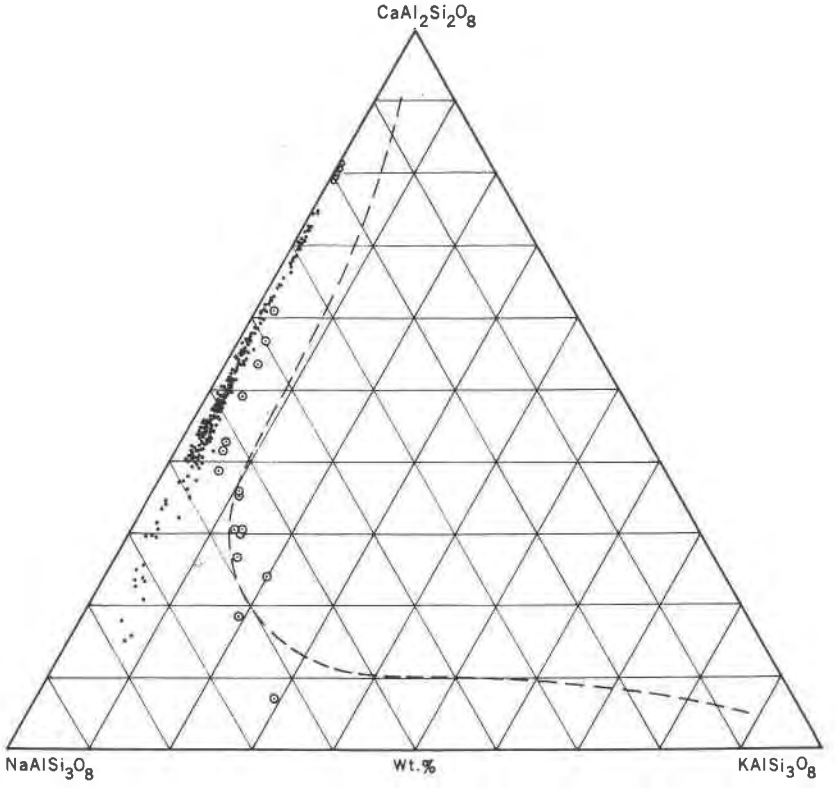

FIG. 8. Compilation of the feldspar data shown for individual rocks in Fig. 7, except that the only phenocrysts plotted (open circles) are those found in the basaltic rocks. The dashed line represents the limit of ternary solid solution in natural feldspars (Smith and MacKenzie 1958).

the modal feldspar with the corresponding equilibrium conditions. Accordingly the equilibrium solidus path for each rock will be a curved path from the composition of the first feldspar to precipitate (phenocrysts) to the composition of the normative feldspar.

In contrast, the extensive zoning of the groundmass plagioclase indicates disequilibrium, and the successive zones of each feldspar trace out a fractionation path on the solidus for each rock. A possible complete solidus fractionation path of the Thingmuli series is represented in Figure 8 which is a compilation of all the feldspar data; the not unreasonable assumption is made that each liquid (rock) is on *one* liquid line of descent controlled by fractionation of the early formed crystals.

It is possible that the trend of the normative feldspar compositions (Fig. 8) illustrate a possible liquidus fractionation path (Carmichael

1963a); if so then it may be seen that the liquids become progressively enriched in the potassium and sodium components of feldspar. However the absence of phenocrysts of a potassic sanidine in all the acid rocks from Iceland examined by the writer indicates that the derivative liquids do not reach the natural equivalent of the two-feldspar surface in the ternary feldspar system (Carmichael 1963a).

Chlorophaeite. This is one of the more conspicuous and common of the secondary minerals found in the Thingmuli series. It is found as a vesicle infilling and may also be spread pervasively throughout the rock, presumably as an alteration product of the interstitial glass. In only three basalts (No. 4, 7 and 8) and one icelandite (No. 16) is chlorophaeite present in sufficient abundance to warrant analysis. The electron-probe analyses are given in Table 5 together with the average of four chlorophaeite analyses taken from Wilshire (1958). This average analysis indicates that much of the iron is present in the ferric state, however the writer was very impressed by the rapid change in color of chlorophaeite from green to black within seconds of exposure of a broken rock surface to the atmosphere. This atmospheric oxidation, and the indication of ferrous iron being dominant in pristine chlorophaeite, would also account for the absence of any evidence of later oxidation of the magnetite in all of the four rocks which contain chlorophaeite (Table 1, Nos. 4, 7, 8 and 16).

TABLE 5. ANALYSES OF CHLOROPHAEITE

	4(G.200)	7(G.99)	8(G.244)	16(G.230)	A
SiO_2	47.7	50.6	46.3	46.4	45.11
TiO_2	0.22	0.17	0.46	0.12	0.29
Al_2O_3	3.84	4.60	5.37	3.71	3.91
Fe_2O_3	34.4	31.7	37.2	36.1	22.13
FeO	—	—	—	—	6.66
MnO	0.18	0.16	0.22	0.51	0.47
MgO	5.76	4.98	4.23	3.06	8.16
CaO	3.04	2.77	2.24	3.17	3.13
Na_2O	0.3	0.3	0.4	0.4	0.55
K_2O	0.1	0.1	0.1	0.2	0.14
H_2O^+	—	—	—	—	8.39
Sum	95.5	95.4	96.0	94.7	98.94

A. Average of chlorophaeite analyses (Wilshire 1958) recalculated to 100 percent, excluding H_2O^- before computing average.

Because of the large amount of water in the chlorophaeite analyses,

much of which is removed by the vacuum system of the electron-probe, their totals are not satisfactory indicators of their quality; however they do not seem too discordant with the published results. There is no evidence of any zoning in the chlorophaeites; all the variation found (2%) may be attributed to routine analytical variation. By and large the chlorophaeite analyses reflect the iron-magnesium ratios of the rocks in which they are found.

Conclusions

In those rocks of this volcanic series which show no evidence of any secondary oxidation or mineralization, only magnetite-rich glass and apatite are common accessory phases; both of these are far too small unfortunately to be analyzed with the electron-probe. The secondary minerals, chlorite, an alteration product of glass (Fawcett 1966), and bowlingite, an alteration product of olivine, have also not been analyzed.

Of all the specimens examined with the electron-probe, most have unmixed spinels indicative of subsequent oxidation (Buddington and Lindsley 1964) (Table 1) and of those with one-phase spinels, four specimens contain chlorophaeite which almost instantaneously oxidizes on exposure to air. Apart from the pitchstone (No. 18), there are therefore only three rocks, all basalts, which give no evidence of any secondary oxidation or mineralization. Even in these three basalts (Carmichael 1964, Table 2, Nos. 5, 9 and 10), it possible that the spinels, although one phase, have been partially oxidized (Akimoto *et al.* 1957), although this may be unlikely. It is therefore inadvisable without thorough petrological examination, to use as a basis for comparison any parameter of basaltic analyses which is affected by the subsequent oxidation of iron. These three basaltic rocks (Nos. 5, 9 and 10) are the only contribution in terms of their norms that can be made from the analytical data of the previous paper (Carmichael 1964) to such studies as Coombs (1963) on the role of pyroxene in basaltic magma.

Acknowledgments

The writer is indebted to Professor B. W. Evans for his continued help and advice in the techniques and use of the electron-probe. Part of this study was supported by a grant (GA-480) from the National Science Foundation.

References

Akimoto, S., T. Katsura and M. Yoshida (1957) Magnetic properties of $TiFe_2O_4$-Fe_3O_4 system and the change with oxidation. *J. Geomag. Geoelect.* **9**, 165–178.

Bowen, N. L. and J. F. Schairer (1935) The system MgO-FeO-SiO_2. *Amer. J. Sci.* **29**, 151–217.

Boyd, F. R. and J. F. Schairer (1964) The system $MgSiO_3$-$CaMgSi_2O_6$. *J. Petrology*, **5**, 275–309.

——— AND J. L. ENGLAND (1965) The rhombic enstatite-clinoenstatite inversion. *Carnegie Inst. Wash. Year Book* **64,** 117–120.

BOTTINGA, Y., A. KUDO AND D. WEILL (1966) Some observations on oscillatory zoning and crystallisation of magmatic plagioclase. *Amer. Mineral.* **51,** 792–806.

BROWN, G. M. (1957) Pyroxenes from the early and middle stages of fractionation of the Skaergaard intrusion, East Greenland. *Mineral. Mag.* **31,** 511–543.

——— AND E. A. VINCENT (1963) Pyroxenes from the late stages of fractionation of the Skaergaard intrusion, East Greenland. *J. Petrology,* **4,** 175–197.

BUDDINGTON, A. F. AND D. H. LINDSLEY (1964) Iron-titanium oxide minerals and synthetic equivalents. *J. Petrology,* **5,** 310–357.

CARMICHAEL, I. S. E. (1960) The pyroxenes and olivines from some Tertiary acid glasses. *J. Petrology,* **1,** 309–336.

——— (1963a) The crystallisation of feldspar in volcanic acid liquids. *Quart. J. Geol. Soc. Lond.* **119,** 95–131.

——— (1963b) The occurrence of magnesian pyroxenes and magnetite in porphyritic acid glasses. *Mineral. Mag.* **33,** 394–403.

——— (1964) The petrology of Thingmuli, a Tertiary volcano in eastern Iceland. *J. Petrology,* **5,** 435–460.

——— (1967) The iron-titanium oxides of salic volcanic rocks and their associated ferromagnesian silicates. *Contrib. Mineral. Petrogr.* **14,** 36–64.

COOMBS, D. S. (1963) Trends and affinities of basaltic magmas and pyroxenes as illustrated on the diopside-olivine-silica diagram. *Mineral. Soc. Amer. Spec. Pap.* **1,** 227–250.

EUGSTER, H. P. AND D. R. WONES (1962) Stability relations of the ferruginous biotite, annite. *J. Petrology* **3,** 82–125.

FAWCETT, J. J. (1965) Alteration products of olivine and pyroxene in basalt lavas from the Isle of Mull. *Mineral. Mag.* **35,** 55–68.

FUDALI, R. F. (1965) Oxygen fugacities of basaltic and andesitic magmas. *Geochim. Cosmochim. Acta,* **29,** 1063–1075.

HESS, H. H. (1941) Pyroxenes of common mafic magmas. *Amer. Mineral.* **26,** 515–535, 573–594.

HOFFER, J. M. (1966) Compositional variations of plagioclase feldspar from a basaltic lava flow. *Amer. Mineral.* **51,** 807–813.

KUNO, H. (1955) Ion substitution in the diopside-ferropigeonite series of clinopyroxenes. *Amer. Mineral.* **40,** 70–93.

——— (1966) Review of pyroxene relations in terrestrial rocks in the light of recent experimental works. *Mineral. J.,* **5,** 21–43.

LINDSLEY, D. H. (1965) Ferrosilite. *Carnegie Inst. Wash. Year Book.* **64,** 148–150.

MCDOUGALL, I. (1961) Optical and chemical studies of pyroxenes in a differentiated Tasmanian dolerite. *Amer. Mineral.* **46,** 661–687.

MOORBATH, S. AND G. P. L. WALKER (1965) Strontium isotope investigation of igneous rocks from Iceland. *Nature,* **207,** 837–840.

MUIR, I. D. AND C. E. TILLEY (1964) Iron enrichment and pyroxene fractionation in tholeiites. *Geol. J.,* **4,** 143–156.

——— AND J. V. P. LONG (1965) Pyroxene relations in two Hawaiian hypersthene-bearing basalts. *Mineral. Mag.* **34,** 358–369.

OSBORN, E. F. (1959) Role of oxygen pressure in the crystallisation and differentiation of basaltic magma. *Amer. J. Sci.* **257,** 609–647.

PECK, D. L. AND T. L. WRIGHT (1966) Experimental studies of molten basalt in situ: A summary of physical and chemical measurements on Recent lava lakes of Kilauea volcano, Hawaii (abstr.). *Ann. Meet. Geol. Soc. Amer.* **1966,** 158–159.

POLDERVAART, A. AND H. H. HESS (1951) Pyroxenes in the crystallisation of basaltic magma. *J. Geol.* **59,** 472–489.

SIMKIN, T. AND J. V. SMITH (1966) Minor element distribution in olivine. *Ann. Meet. Geol. Soc. Amer.* **1966,** 203.

SMITH, J. V. AND W. S. MACKENZIE (1958) The alkali feldspars: IV The cooling history of high-temperature sodium-rich feldspars. *Amer. Mineral.* **43,** 872–889.

TILLEY, C. E., H. S. YODER AND J. F. SCHAIRER (1963) Melting relations of basalts. *Carnegie Inst. Wash. Year Book* **62,** 77–84.

VINCENT, E. A. AND R. PHILLIPS (1954) Iron-titanium oxide minerals in layered gabbros of the Skaergaard intrusion, East Greenland. *Geochim. Cosmochim. Acta.* **6,** 1–26.

WAGER, L. R. (1960) The major element variation of the layered series of the Skaergaard intrusion and a re-estimation of the average composition of the hidden layered series and of the succesive residual magmas. *J. Petrology,* **1,** 364–398.

——— AND W. A. DEER (1939) Geological investigations in East Greenland. Part III. The petrology of the Skaergaard intrusion, Kangerdlugssuak. *Medd. Gronland* **105,** 1–352.

WILSHIRE, H. G. (1958) Alteration of olivine and orthopyroxene in basic lavas and shallow intrusions. *Amer. Mineral.* **43,** 120–147.

WONES, D. R. AND H. P. EUGSTER (1965) Stability of biotite: experiment, theory and application. *Amer. Mineral.* **50,** 1228–1272.

YODER, H. S., C. E. TILLEY AND J. F. SCHAIRER (1963) Pyroxenes and associated minerals in the crust and mantle. *Carnegie Inst. Wash. Year Book* **62,** 84–94.

Manuscript received, February 20, 1967; accepted for publication September 29, 1967.